Notes

Core−Sheath Nanofibers from Combined Atom Transfer Radical Polymerization and Electrospinning

G. D. Fu,* J. Y. Lei, C. Yao, X. S. Li, and F. Yao

School of Chemistry and Chemical Engineering, Southeast University, Jianging District, Nanjing, Jiangsu P. R. China 211189

S. Z. Nie

Suzhou Institute of Sichuan University, No. 188 Ren'ai Rd., Suzhou Industrial Park, Jiangsu, P. R. China 215123

E. T. Kang and K. G. Neoh

Department of Chemical & Biomolecular Engineering, National University of Singapore, Kent Ridge, Singapore 119260

Received March 5, 2008
Revised Manuscript Received May 21, 2008

Introduction

Surface-functionalized polymeric nanofibers, especially those with a core−sheath structure, are of growing interest for their potential applications in tissue engineering,[1,2] biosensor technology,[3] drug delivery,[4] and nanotube fabrication.[5] Core−sheath polymeric nanofibers have been prepared by a template-directed approach[5,6] and by coaxial electrospinning.[7−12] Electrospinning generates fibers by accelerating a jet of charged polymer solution or polymer melt in an electric field.[13,14] Electrospinning is becoming an attractive approach to the preparation of continuous micrometer-scale to submicrometer-scale fibers in both university and industry for its applicability to a wide range of materials.[15] Recently, core−sheath nanofibers have been prepared via electrospinning of block copolymers.[12,16,17] Nanofibers with enriched selective segments or blocks on the surface are obtained arising from the difference in surface energy[16,17] and polarity[12] between the two types of blocks.

Surface-initiated atom transfer radical polymerization (ATRP) is an good approach for preparing dense and uniform polymer brushes on various substrates, such as polymer,[18,19] silica particles,[20−22] gold particles,[22,24] and carbon nanotubes.[25] When the substrates were nanoparticles or nanorods, core−shell nanostructures were obtained due to the presence of a high density of polymer brushes from ATRP.[21,22] The mechanism of ATRP involves a rapid dynamic equilibrium between a minute amount of growing free radicals and a large amount of dormant species.[26−28] The resulting polymers with "dormant" end groups can be used as macroinitiators to synthesize block copolymers. This study reports the effect of electrospinning on the dormant alkyl halide species (ATRP macroinitiators). The core−sheath nanofibers were prepared by electrospinning, under different conditions, of polystyrene synthesized via ATRP, followed by surface-initiated ATRP of acrylamide (AAM) or *N*-(hydroxylmethyl)acrylamide (HMAM). The experimental procedures are shown in Scheme 1.

Results and Discussion

In order to study the effect of electrospinning on the dormant alkyl halide chain ends of polymers, α-methylbenzyl bromide (MBB) was used to initiate atom transfer radical polymerization (ATRP) of styrene. Thus, there are no other functional groups except alkyl bromide in the polystyrene (PS) macromolecule. Table 1 shows PS samples of different molecular weights prepared from ATRP. PS fibers with diameter in the range of 10−1000 nm can be easily prepared by electrospinning.[29−31] Figure 1a shows the scanning electron microscope (SEM) image of PS nanofibers electrospun from a 10 wt % dimethylformamide (DMF):tetrahydrofuran (THF) (DMF:THF = 2:1 in volume ratio) mixed solution of PS1 (number-average molecular weight, $M_n = 5.9 \times 10^3$ g/mol, and polydispersity index, PDI = 1.21, Table 1), with the cathode positioned at spinneret side ($PS_{n\text{-}c}$). The nanofibers are uniform and have a diameter in the range of 400−500 nm.

The surface bromide (Br) concentration of $PS_{n\text{-}c}$, the corresponding PS nanofibers electrospun with the anode positioned at the spinneret side ($PS_{n\text{-}a}$), and the corresponding PS film cast from the same PS1 solution were studied by X-ray photoelectron spectroscopy (XPS). Table 1 summarizes the surface Br concentrations of the PS films and $PS_{n\text{-}c}$ and $PS_{n\text{-}a}$ nanofibers. The surface Br concentrations of the PS films and $PS_{n\text{-}a}$ nanofibers are very close to the theoretical value of the original polymer. For the PS1 polymer in Table 1, the Br content of the corresponding $PS_{n\text{-}a}1$ nanofibers is about of 0.28 atom %, which is very close to that of the PS1 film (0.21%) and the theoretical value (0.22%). The XPS results suggest that the dormant alkyl halide species at the PS chain ends is well preserved on the resulting fiber surfaces, when electrospinning is carried out with the anode positioned at the spinneret. The XPS results in Table 1 also indicate that the surface Br concentration of $PS_{n\text{-}c}$ nanofibers is much higher than that of the corresponding PS film and $PS_{n\text{-}a}$ nanofibers. The surface Br concentration of $PS_{n\text{-}c}$ nanofibers electrospun from PS1 polymer is about 0.56 atom %, which is much higher than that of the PS1 film and $PS_{n\text{-}a}1$ nanofibers. During the electrospinning process, polymer fluids are exposed to a high electrical potential. Electrical charges were generated on the surface of polymer fluids.[32] For the DMF:THF mixed solution of PS, DMF is the main charge carrier because DMF has a dielectric constant of about 37, which is much higher than that (2.5) of PS and that (7.5) of THF.[33] Since the alkyl bromide group (C−Br) is a polar (electronegative) species, the Br atom can acquire a partial negative charge (δ^-). When PS was electrospun with the cathode positioned at the spinneret, the polymer fluids become positively charged on the surface. The positive charges will drive the alkyl bromide groups to the surface by electrostatic attraction (Scheme 1). With the evaporation of solvents during the flight of the fluid jet to the

* To whom correspondence should be addressed: Tel +86-25-52090625; Fax +86-25-52090621, e-mail fu7352@seu.edu.cn.

10.1021/ma800499h CCC: $40.75
Published on Web 08/20/2008

Scheme 1. Preparation of Core−Sheath Nanofibers from Electrospinning, in Which the Alkyl Bromide Groups of PS Migrate to the Liquid Surface under Electrostatic Attraction, and Surface-Initiated ATRP[a]

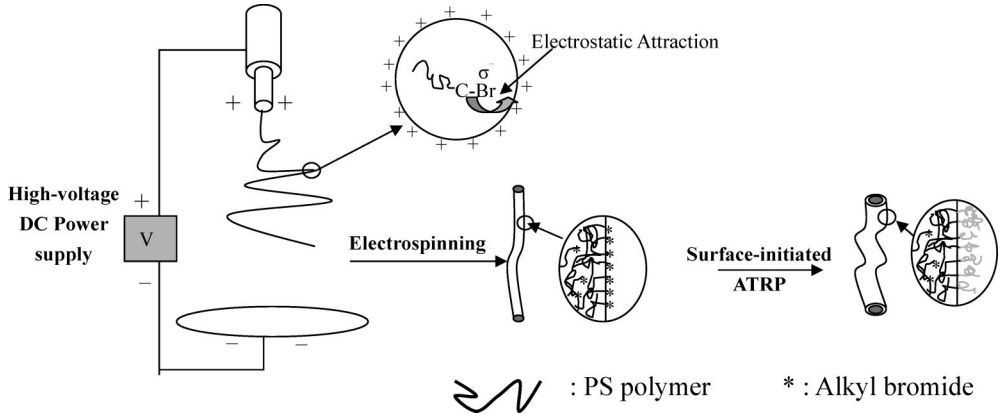

[a] ATRP = atom transfer radical polymerization; PS = polystyrene.

Table 1. Characterization of Polystyrene (PS) Nanofiber Prepared by Electrospinning

				bromo content atomic concentration (%) aromatic content				diameters[f] (nm)	
sample	reaction time (h)	$M_n \times 10^3$ (g/mol)	PDI	theoretical value[b]	cast film[c]	$PS_{n\text{-}a}$ fiber[d]	$PS_{n\text{-}c}$ fiber[e]	$PS_{n\text{-}a}$ fiber	$PS_{n\text{-}c}$ fiber
PS 1[a]	1	5.9	1.21	0.22	0.21	0.28	0.56	450 ± 18	430 ± 20
PS 2	2	9.8	1.19	0.13	0.15	0.11	0.38	250 ± 16	240 ± 13
PS 3	4	15.0	1.18	0.09	0.08	0.10	0.18	140 ± 17	160 ± 10
PS 4	8	33.3	1.24	0.04	0.06	0.07	0.14	80 ± 12	60 ± 15

[a] The α-methylbenzyl bromide (MBB) was used as the initiator. The molar ratio of [styrene]:[MBB]:[CuBr]:[bpy] = 400:1:1:3; bpy = 2,2′-bipyridine. [b] The theoretical value of bromo content of PS was calculated according to the equation $1/[M_n \times 8/104]$, in which M_n is the molecular weight of PS,104 is the molecular weight of styrene, 8 accounts for the eight carbon atoms in styrene, and assuming there is one bromine atom in each PS chain. [c] The PS film was obtained by casting a 10 wt % DMF:THF (volume ratio 2:1) mixed solution of PS. DMF = dimethylformide, THF = tetrahydrofuran. [d] XPS results of nanofibers electrospun from a 10 wt % DMF:THF (volume ratio 2:1) mixed solution with the cathode positioned at spinneret side. [e] XPS results from nanofibers electrospun from a 10 wt % DMF:THF (volume ratio 2:1) mixed solution with the anode positioned at spinneret side. [f] Average diameter of 50 nanofibers determined from scanning electron microscope (SEM) images.

collector and the solidification of the PS nanofibers, PS nanofibers with surface-enriched alkyl bromide groups are produced. For the nanofibers electrospun with an anode positioned at spinneret, the electrostatic attraction will not occur. Thus, the alkyl bromide groups are randomly distributed on the surface and in the matrix of the fibers, just like the PS film cast from the DMF:THF solution.

Surface-initiated ATRP of acrylamide (AAM) and *N*-(hydroxymethyl)acrylamide (HMAM) from PS films and $PS_{n\text{-}c}$ and $PS_{n\text{-}a}$ nanofibers were carried out in aqueous solutions at ambient temperature. Since PS is hydrophobic, the nanofiber will remain intact as a heterogeneous phase during the ATRP in an aqueous medium. Most importantly, only those alkyl bromide groups on the fiber surface can initiate the ATRP of hydrophilic monomers. Figure 1b shows the SEM image of the $PS_{n\text{-}c}$ nanofibers with surface-grafted AAM polymer (PAAM), or the $PS_{n\text{-}c}$-*g*-PAAM nanofibers, after 4 h of surface-initiated ATRP of AAM from $PS_{n\text{-}c}$ nanofibers electrospun from PS1 in Table 1. The SEM image suggests that the nanostructure of the fibers is well-preserved. Figures 2a−c show the respective C 1s core-level spectra of PS-*g*-PAAM film, $PS_{n\text{-}a}$-*g*-PAAM nanofibers, and $PS_{n\text{-}c}$-*g*-PAAM nanofibers, prepared from PS1 in Table 1. The C 1s core-level spectra are curved-fitted with three peak components, with bonding energies (BEs) at 284.6 eV for the *C*−H species, at 287.8 eV for the *C*═O species, and at 291.4 eV for the $\pi-\pi^*$ shakeup satellite of the aromatic rings.[34,35] The presence of *C*═O species at the BE of 287.8 eV indicates that the PAAM brushes has been successfully grafted on the PS film and the $PS_{n\text{-}a}$ and $PS_{n\text{-}c}$ nanofibers. The [C]/[O] molar ratio of the $PS_{n\text{-}a}$-*g*-PAAM fibers, derived from XPS results, is about 10.3, which is comparable to that (9.4) of the PS-*g*-PAAM film. The [C]/[O] molar ratio of $PS_{n\text{-}c}$-*g*-PAAM fibers is about 3.2, which is close to the theoretical value (3.0) of PAAM. In Figure 2c, the substantial increase in the intensity of *C*═O species and the disappearance of $\pi-\pi^*$ shakeup satellite signal of the aromatic rings of PS at the BE of 291.4 eV suggest that the surfaces of $PS_{n\text{-}c}$-*g*-PAAM nanofibers are completely covered by the PAAM brushes to a thickness greater than the probing depth of the XPS technique (~8 nm in an organic matrix[21]). Thus, a core−sheath structure must have formed.

Since ATRPs were carried out under the same reaction conditions, the lengths of PAAM brushes on the planar PS-*g*-PAAM film and the $PS_{n\text{-}a}$-*g*-PAAM and $PS_{n\text{-}c}$-*g*-PAAM nanofibers should be comparable. The XPS results reveal that the PAAM brushes on the $PS_{n\text{-}c}$-*g*-PAAM nanofiber surface are denser than those on the $PS_{n\text{-}a}$-*g*-PAAM nanofiber and PS film surfaces (Scheme 2). Figures 2d−f show the C 1s core-level spectra of the PS-*g*-PHMAM film and $PS_{n\text{-}a}$-*g*-PHMAM and $PS_{n\text{-}c}$-*g*-PHMAM nanofibers, prepared from PS1 polymer in Table 1. The C 1s core-level spectra are curved-fitted into four peak components, with BE at 284.6 eV for the *C*−H species, at 286.1 eV for the *C*−O species, at 287.8 eV for the *C*═O species, and at 291.4 eV for the $\pi-\pi^*$ shakeup satellite of the aromatic rings.[34,35] The presence of *C*−O species at the BE of 286.1 eV and *C*═O species at the BE of 287.8 eV indicates that the PHMAM brushes have been successfully grafted on the PS film and PS nanofibers. The XPS results also suggest that the PHMAM brushes on the $PS_{n\text{-}c}$-*g*-PHMAM nanofiber surface are much denser than those on the PS-*g*-PHMAM film and $PS_{n\text{-}a}$-*g*-PHMAM nanofiber surfaces. This result is again consistent with the fact that the $PS_{n\text{-}c}$ nanofibers have a higher concentration of alkyl bromide groups on the surface.

The successful preparation of core−sheath PS-*g*-PAAM and PS-*g*-PHMAM nanofibers was also confirmed by the measure-

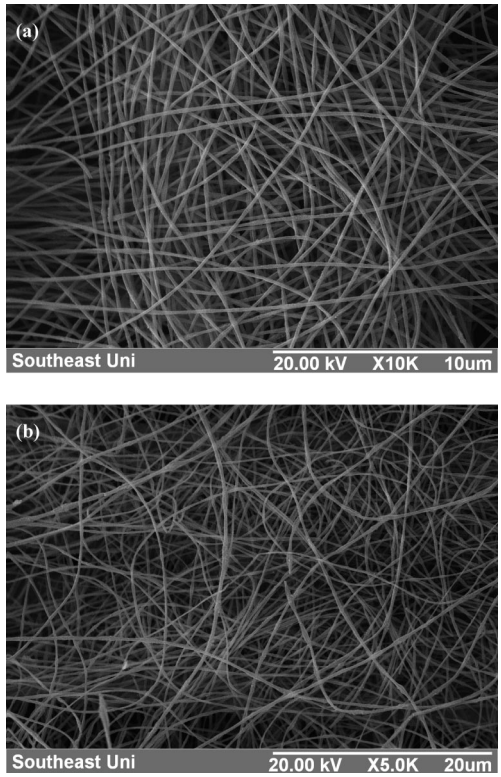

Figure 1. Scanning electron microscope (SEM) surface images of the (a) $PS_{n\text{-}c}$ nanofibers electrospun from a 10 wt % DMF:THF (DMF:THF = 2:1 in volume ratio) mixed solution of PS1 in Table 1, with cathode positioned at the spinneret, and (b) the $PS_{n\text{-}c}$ nanofibers after 4 h of surface-initiated atom transfer radical polymerization (ATRP) of AAM (AAM = acrylamide, DMF = dimethylformamide, THF = tetrahydrofuran).

ment of the water contact angles. Table 2 summarizes the water contact angles of nanofibers. The water contact angle of PS1 nanofibers is of about 130°. The large water contact angle of the PS nanofibers is attributable to the surface roughness of PS nanofibers in the aggregate and the hydrophobicity of PS. All the PS-*g*-PHMAM and PS-*g*-PAAM nanofibers in the aggregate exhibit substantially smaller advancing and receding water contact angles. Table 2 also shows that the respective advancing water contact angles (θ_a) of $PS1_{n\text{-}c}$-*g*-PAAM and $PS1_{n\text{-}c}$-*g*-PHMAM nanofibers in the aggregate are 30° and 42°, which are much lower than those of their $PS1_{n\text{-}a}$-*g*-PAAM (62°) and $PS1_{n\text{-}a}$-*g*-PHMAM (83°) counterparts. The more hydrophilic nature of the $PS_{n\text{-}c}$-*g*-PAAM and $PS_{n\text{-}c}$-*g*-PHMAM nanofibers is consistent with the presence of denser polymer brushes on their surfaces. Attempts were made, in vain, to characterize the core−sheath structure of the nanofibers by transmission electron microscope (TEM). Presumably there is a lack of sufficient contrast in electron beam images between the PS and PAAM or PHMAM polymers of comparable mass density.

Conclusions

A simple method for preparing core−sheath nanofibers via combined bulk atom transfer radical polymerization (ATRP), electrospinning, and surface-initiated ATRP has been developed. By carefully selecting the electrospinning conditions, PS nanofibers with surface-enriched ATRP initiator sites can be obtained. Subsequent surface-initiated ATRP allows the preparation of core−sheath nanofibers. Because of applicability of ATRP to a wide selection of functional monomers, core−sheath fibers with diameter ranging from nanoscale to microscale and with various functionalities can be readily prepared. The present method also

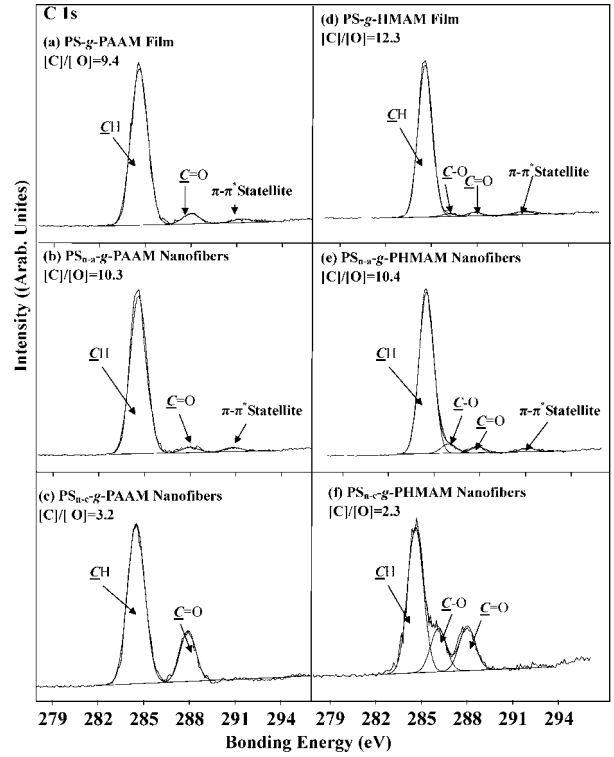

Figure 2. X-ray photoelectron spectroscopy (XPS) C 1s core-level spectra of the (a) polystyrene-*graft*-poly(acrylamide) (PS-*g*-PAAM) film, (b) $PS_{n\text{-}a}$-*g*-PAAM nanofibers, (c) $PS_{n\text{-}c}$-*g*-PAAM nanofibers, (d) PS-*g*-PHMAM film, (e) $PS_{n\text{-}a}$-*g*-PHMAM nanofibers, and (f) $PS_{n\text{-}c}$-*g*-PAAM nanofibers, prepared from a 10 wt % mixed DMF:THF (DMF:THF = 2:1, volume ratio) mixed solution of PS1 in Table 1 (DMF = dimethylformamide; THF = tetrahydrofuran; $PS_{n\text{-}a}$ = nanofibers of polystyrene (PS) electrospun with anode positioned at the spinneret; $PS_{n\text{-}c}$ = nanofibers of PS electrospun with cathode positioned at the spinneret; PMMA = polyacrylamide; PHMAM = poly(*N*-(hydroxymethyl)acrylamide)).

provides a possibility for preparing nanotubes via the preparation of core−sheath nanofibers and subsequent selective removal of the core. Arising from the narrow polydispersity index of the macromolecules from ATRP, the sheath thickness of the nanofibers or the shell thickness of the nanotubes could be defined and controlled by simply regulating the polymerization time.

Experimental Section

Materials. The monomers, styrene (99%), *N*-(hydroxylmethyl)acrylamide (HMAM, 98%), and acrylamide (AAM, 99%) were purchased from Sinopharm. Chem. Reagent Co. Ltd., China. α-Methylbenzyl bromide (MBB, 97%), copper bromide(I) (CuBr, 99.9%), *N*,*N*,*N*′,*N*′,*N*″-pentamethyldiethlyenetriamine (PMDETA, 99%), and 2,2′-bipyridine (bpy, 99.5%) were purchased from Shanghai Chemical Reagent Plant, Shanghai, China. The analytical grade of tetrahydrofuran (THF) and dimethylformamide (DMF) was also purchased from Shanghai Chemical Reagent Plant, Shanghai, China, and used as received.

Atom Transfer Radical Polymerization (ATRP) of Styrene. MBB (14 μL, 0.1 mmol), CuBr (14.3 mg, 0.1 mmol), and styrene (1.2 mL, 0.01 mol) were introduced into a Pyrex test tube equipped with a magnetic stirrer. The reaction mixture was degassed by bubbling argon for 20 min, after which 0.048 g (0.3 mmol) of bpy was added to the mixture under an argon atmosphere. The reaction mixture was flushed with argon for another 10 min, and the test tube was sealed tightly with a rubber stopper. Polymerization was carried out under continuous stirring at 110 °C. After 120 min, the reaction mixture turned viscous, and the reaction was stopped by diluting with THF. The catalyst complex was removed from the

Scheme 2. Schematic Illustration of the Difference in Density of Polymer Brushes via Surface-Initiated ATRP from a $PS_{n\text{-}a}$ and $PS_{n\text{-}c}$ Nanofiber[a]

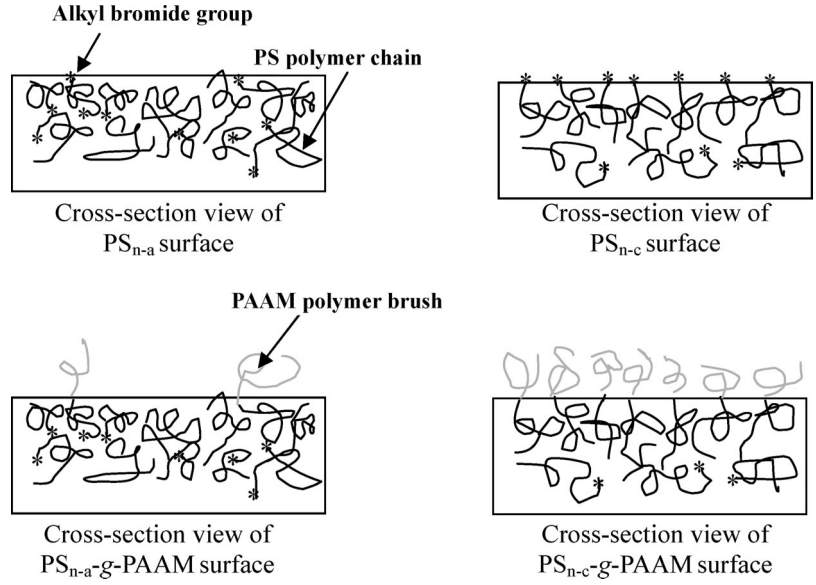

[a] ATRP = atom transfer radical polymerization; $PS_{n\text{-}a}$ = nanofibers of polystyrene (PS) electrospun with anode positioned at the spinneret; $PS_{n\text{-}c}$ = nanofibers of PS electrospun with cathode positioned at the spinneret; PAAM = poly(acrylamide); $PS_{n\text{-}a}$-*g*-PAAM = $PS_{n\text{-}a}$-*graft*-poly(*N*-(hydroxylmethyl)acrylamide); $PS_{n\text{-}c}$-*g*-PAAM = $PS_{n\text{-}c}$-*graft*-poly(*N*-(hydroxylmethyl)acrylamide)).

Table 2. Characterization of the Polystyrene-*graft*-poly(acrylamide) (PS-*g*-PAAM) and Polystyrene-*graft*-poly(*N*-(hydroxylmethyl)acryamide) (PS-*g*-PHMAM) Nanofibers

			water contact angle[d]	
sample	polymerization time (h)	diameter[c] (nm)	θ_A	θ_R
PS film			96 ± 2	61 ± 3
$PS1_{n\text{-}a}$		450 ± 18	128 ± 3	90 ± 3
$PS1_{n\text{-}c}$		430 ± 20	134 ± 3	96 ± 2
$PS1_{n\text{-}a}$-*g*-PAAM[a]	4	440 ± 19	62 ± 3	43 ± 3
$PS1_{n\text{-}c}$-*g*-PAAM[a]	4	445 ± 19	30 ± 2	15 ± 4
$PS1_{n\text{-}a}$-*g*-PHMAM[b]	4	460 ± 14	83 ± 4	52 ± 5
$PS1_{n\text{-}c}$-*g*-PHMAM[b]	4	455 ± 16	42 ± 3	36 ± 4
$PS2_{n\text{-}a}$-*g*-PAAM[a]	4	255 ± 12	82 ± 4	38 ± 6
$PS2_{n\text{-}c}$-*g*-PAAM[a]	4	251 ± 14	31 ± 5	14 ± 3
$PS2_{n\text{-}a}$-*g*-PHMAM[b]	4	250 ± 13	78 ± 3	43 ± 2
$PS2_{n\text{-}c}$-*g*-PHMAM[b]	4	253 ± 11	33 ± 2	16 ± 3
$PS3_{n\text{-}a}$-*g*-PAAM[a]	4	170 ± 15	72 ± 2	28 ± 4
$PS3_{n\text{-}c}$-*g*-PAAM[a]	4	153 ± 21	29 ± 3	12 ± 3
$PS3_{n\text{-}a}$-*g*-PHMAM[b]	4	168 ± 13	79 ± 3	23 ± 2
$PS3_{n\text{-}c}$-*g*-PHMAM[b]	4	146 ± 16	21 ± 2	14 ± 3

[a] Surface-initiated atom transfer radical polymerization (ATRP) of nanofibers electrospun from PS samples in Table 1 were carried out at room temperature in aqueous solution containing 7.2 mg of CuBr, 2.9 g of acrylamide, 14 μL of PMEDTA, and 5 mL of double-distillated water. CuBr = copper(I) bromide, PMEDTA = *N*,*N*,*N*′,*N*′,*N*″-pentamethyldiethlyenetriamine. [b] Surface-initiated ATRP of nanofibers electrospun from PS samples in Table 1 were carried out at room temperature in aqueous solution containing 7.2 mg of CuBr, 3.0 g of HMAM, 14 μL of PMEDTA, and 5 mL of double distillated water. HMAM = *N*-(hydroxylmethyl)acrylamide. [c] Average diameter of 50 nanofibers determined from scanning electron microscope (SEM) images. [d] θ_A and θ_R are the advancing and receding water contact angle, respectively, in degrees. The value is the average of five measurements.

reaction mixture by passing the mixture through an alumina column. The polystyrene (PS) homopolymer was precipitated in an excess volume of methanol and recovered by filtration. After drying under reduced pressure overnight, 0.55 g of white polymer powders was obtained (number-average molecular weight, $M_n = 5.9 \times 10^3$ g/mol, and polydispersity index, PDI = 1.21).

Preparation of PS Film. PS was dissolved in a DMF:THF (volume ratio 2:1) mixed solvent to a concentration of 10 wt %. PS films with a thickness of about 1−2 μm were obtained by spinning-coating from the solution at 500 round/min on a clean glass slide. The film was then kept at 80 °C for 6 h and then at 120 °C for another 3 h in a vacuum oven.

Electrospinning. PS was dissolved in a DMF:THF (volume ratio 2:1) mixed solvent to a concentration of 10 wt %. In an electrospinning unit, the PS solution was fed at a constant rate of 6 mL/h to a syringe by a digitally controlled micropump. The tip of the syringe was connected to a high-voltage supply (Tianjing Dongwen High Voltage Electronics Inc.). Electrospinning was carried out at an electrical potential of 10 kV using a needle with an inner diameter of about 0.6 mm. The distance between the tip of the needle and the grounded collector was fixed at about 20 cm. All electrospinning was carried out at room temperature. The obtained PS nanofibers were dried under reduced pressure overnight.

Surface-Initiated ATRP. CuBr (7.2 mg, 0.05 mmol), AAM (2.9 g, 0.04 mol), and 5 mL of double distillated water were introduced into a Pyrex test tube. The reaction mixture was degassed by bubbling argon for 20 min, after which 14 μL (0.05 mmol) of PMEDTA was introduced into the mixture under an argon atmosphere. After purging with argon for another 10 min, about 0.1 g of nanofibers of PS electrospun with anode positioned at the spinneret ($PS_{n\text{-}c}$) was added, and the tube was sealed with a rubber stopper. The reaction was allowed to process for 4 h. Then, the nanofibers were carefully removed from solution and rinsed with water and ethanol thrice. After drying under the reduced pressure for 12 h, 0.121 g of the nanofibers was obtained. The surface-initiated ATRP of HMAM from $PS_{n\text{-}c}$ nanofibers was carried under the same reaction conditions, except HMAM monomer was used. After 4 h of reaction, 0.126 g of the nanofibers was obtained.

Characterization. Gel permeation chromatography (GPC) was performed on an HP 1100 high-pressure liquid chromatograph (HPLC) equipped with an HP 1047A refractive index detector and a PLgel MIXED-C 300−7.5 mm column. The column packing allowed the separation of polymers over a wide molecular weight range of 200−3 000 000. THF was used as the eluent at a low flow rate of 1 mL/min at 35 °C. Polystyrene molecular weight standards were used as the references. XPS measurements were carried out on a Kratos AXIS HSi spectrometer (Kratos Analytical Ltd.,

Manchester, England) with a monochromatized Al Kα X-ray source (1486.6 eV photons). The X-ray source was run at a reduced power of 150 W (15 kV and 10 mA). The samples were mounted on the standard sample studs by means of double-sided adhesive tapes. The core-level spectra were obtained at the photoelectron takeoff angle (with respect to the sample surface) of 90°. The pressure in the analysis chamber was maintained at 10^{-8} Torr or lower during sample measurements. Surface elemental stoichiometries were determined from the spectral area ratios, after correcting with the experimentally determined sensitivity factors, and were reliable to within ±10%. Scanning electron microscopy measurements were carried out on an electron microscope (Hitachi X-650 SEM) at an accelerating voltage of 5−20 kV and an object distance of about 8 mm. The advancing and receding water contact angles were measured at 25 °C and 50% relative humidity on a telescopic goniometer (Rame-Hart, model 100-00(230), Moutain Lake, NJ). The telescope with a magnification power of 23× was equipped with a protractor of 1° graduation. For each angle reported, at least five readings from different surface locations were averaged.

Acknowledgment. This work was supported by Southeast University Foundation Grants 4007041012 and 4007041023. We are also grateful for the support of the Nanjing City Returning Scholar Foundation under Grant 7607044041 and the Key Project of the Chinese Ministry of Education Grant 108062.

References and Notes

(1) Langer, R.; Vacanti, J. P. *Science* **1993**, *260*, 920–926.
(2) Koh, C. J.; Atala, A. *J. Am. Soc. Nephrol.* **2004**, *15*, 1113–1125.
(3) Chang, Y. J.; Chen, Y. C.; Kuo, H. L.; Wei, P. K. *J. Biomed. Opt.* **2006**, *11*, Art. No. 014032.
(4) Scoppimath, K. S.; Aminabhavi, T. M.; Kulkarni, A. R.; Rudzinski, W. E. *J. Controlled Release* **2001**, *70*, 1–20.
(5) Hou, H.; Jun, Z.; Reuning, A.; Schaper, A.; Wendorff, J. H.; Greiner, A. *Macromolecules* **2002**, *35*, 2429–2431.
(6) Crauso, R. A.; Schattka, J. H.; Greiner, A. *Adv. Mater.* **2001**, *13*, 1577.
(7) Kalra, V.; Mendez, S.; Lee, J. H.; Nguyen, H.; Marquez, M.; Joo, Y. L. *Adv. Mater.* **2006**, *18*, 3299–3303.
(8) Sun, Z.; Zussman, E.; Yarin, A. L.; Wendorff, J. H.; Greiner, A. *Adv. Mater.* **2003**, *15*, 1929–1932.
(9) Larsen, G.; Velarde-Ortiz, R.; Minchow, K.; Barrero, A.; Loscertales, I. G. *J. Am. Chem. Soc.* **2003**, *125*, 1154–1155.
(10) Li, D.; Xia, Y. *Nano Lett.* **2004**, *4*, 933–938.
(11) Ma, M.; Krikorian, V.; Yu, J. H.; Thomas, E. L.; Rutledge, G. C. *Nano Lett.* **2006**, *12*, 2969–2972.
(12) Sun, X. Y.; Shankar, R.; Borner, H. G.; Chosh, T. K.; Spontak, R. *Adv. Mater.* **2007**, *19*, 87–91.
(13) Fridrick, S. V.; Yu, J. H.; Brenner, M. P.; Rutledge, G. C. *Phys. Rev. Lett.* **2003**, *90*, 144502-1–144502-4.
(14) Greiner, A.; Wendorff, J. H. *Angew. Chem., Int. Ed.* **2007**, *46*, 5670–5703.
(15) Ramakrishna, S.; Fujihara, K.; Teo, W. E.; Yong, T.; Ramaseshan, R. *Mater. Today* **2006**, *9*, 40–50.
(16) Brantley, E. L.; Jennings, G. K. *Macromolecules* **2004**, *37*, 1476–1483.
(17) Ma, M.; Hill, R. M.; Lowery, J. L.; Fridrikh, S. V.; Rutledge, G. C. *Langmuir* **2005**, *21*, 5549.
(18) Deitzel, J. M.; Kosik, W.; McKnight, S. H.; Beck Tan, N. C.; Desimone, J. M.; Crette, S. *Polymer* **2002**, *43*, 1025.
(19) Desai, S. M.; Solanky, S. S.; Mandale, A. B.; Rathore, K.; Singh, R. P. *Polymer* **2003**, *44*, 7645–7649.
(20) Edmondson, S.; Vo, C. D.; Armes, S. P.; Unali, G. F. *Macromolecules* **2007**, *40*, 5271–5278.
(21) Fu, G. D.; Zhao, J. P.; Sun, Y. M.; Kang, E. T.; Noeh, K. G. *Macromolecules* **2007**, *40*, 2271–2275.
(22) Fu, G. D.; Shang, Z. H.; Hong, L.; Kang, E. T.; Neoh, K. G. *Adv. Mater.* **2005**, *17*, 2622–2625.
(23) Lou, X. H.; He, L. *Langmuir* **2006**, *22*, 2640–2646.
(24) Bhat, R. R.; Tomlinson, M. R.; Genzer, J. *Macromol. Rapid Commun.* **2004**, *25*, 270–274.
(25) Kong, H.; Gao, C.; Yan, D. Y. *Macromolecules* **2004**, *37*, 4022–4030.
(26) Matyjaszewski, K.; Xia, J. H. *Chem. Rev.* **2001**, *101*, 2921–2990.
(27) Kamigaito, M.; Ando, T.; Sawanmoto, M. *Chem. Rev.* **2001**, *101*, 3689–3745.
(28) Braunecker, W. A.; Matyjaszewski, K. *Prog. Polym. Sci.* **2007**, *32*, 93–146.
(29) Fantini, D.; Zanetti, M.; Costa, L. *Macromol. Rapid Commun.* **2006**, *27*, 2038–2042.
(30) Wang, C.; Hsu, C. H.; Lin, J. H. *Macromolecules* **2006**, *39*, 7662–7672.
(31) Pattamaprom, C.; Hongrojjanawiwat, W.; Koombhongse, P. *Macromol. Mater. Eng.* **2006**, *291*, 840–847.
(32) Fridrikh, S. V.; Yu, J. H.; Brenner, M. P.; Rutldge, G. C. *Phys. Rev. Lett.* **2003**, *90*, 144502-1.
(33) Wannatong, L.; Sirvat, A.; Supaphol, P. *Polym. Int.* **2004**, *53*, 1851–1859.
(34) Beamson, G.; Briggs, D. *High Resolution XPS of Organic Polymers. The scienta ESCA 300 Database*; John Wiley & Son: Chichester, 1992; p 274.
(35) Muilenberg, G. E., Ed.; *Handbook of X-ray Photoelectron Spectroscopy*; Perkin-Elmer: Eden Prairie, MN, 1978; p 94.

MA800499H